

A compact physical model for morphology induced intrinsic degradation of organic bulk heterojunction solar cell

Biswajit Ray^{a)} and Muhammad A. Alam^{b)}

School of Electrical and Computer Engineering, Purdue University, West Lafayette, Indiana 47906, USA

(Received 9 November 2010; accepted 22 June 2011; published online 19 July 2011)

The gradual loss of efficiency during field operation poses a fundamental challenge for economic viability of any solar cell technology. Well known examples include light-induced degradation in Si-based cell (Staebler-Wronski effect), Cu diffusion in thin film (copper indium gallium selenide) cell, hot-spot degradation in series connected modules, etc. Here we develop a compact model for an intrinsic degradation concern for bulk heterojunction type organic photovoltaic (BH-OPV) cells that involve continued (thermal) phase segregation of the donor-acceptor molecules leading to characteristic loss of efficiency and performance. Our approach interprets a number of BH-OPV device degradation measurements within a common framework and suggests/rationalizes intuitive routes for lifetime improvement for such technologies. © 2011 American Institute of Physics. [doi:10.1063/1.3610460]

Bulk heterojunction type organic photovoltaic cell (BH-OPV) has an important advantage of economical processing, which is unfortunately counterbalanced by relatively low power conversion efficiency and poor device stability. There have been significant improvements in the cell efficiency over the last decade (currently >8%, Ref. 1). However, the real bottleneck in the path of successful commercialization of this technology is not the efficiency but its poor operational lifetime,² the theory of which has received relatively little attention so far. As a result, despite significant progress in the power conversion efficiency, the lifetime of BH-OPV lags far behind the inorganic counterparts (typically more than 20 years).

A careful survey of the BH-OPV literature shows that the degradation mechanisms of BH solar cell are complex, diverse, and poorly understood. In a recent review,³ Krebs describes many “extrinsic” degradation mechanisms of BH-OPV, including chemical degradation of electrode metals⁴ and polymer molecules in the presence of oxygen and water,⁵ photo-oxidation of polymers,⁶ thermal degradation due to morphological change,^{7–9} etc. Like any other commercial technology, the extrinsic degradation issues must be addressed by a combination of improved manufacturing techniques and better encapsulation, and there has been sustained progress in this regard over the last few years.¹⁰ On the other hand, “intrinsic degradation” of a solar cell implies that even if the cells were perfectly encapsulated and manufactured for highest yield, the cell performance can still degrade due to the intrinsic morphological change induced by operating (thermal) environment.⁷ Thus, thermal degradation is a fundamental stability concern for BH-OPV, and yet there is no compact theoretical framework to explore the problem quantitatively.

The key contribution in this Letter is the development of a physical degradation model that can relate the intrinsic lifetime of the cell to the constituent material parameters and process conditions. The model is based on the general principle of coarsening kinetics in any phase segregating system,

and hence it is applicable to wide variety of BH-OPV material system (polymer:fullerene, polymer:polymer, etc). We verify our model by analyzing a number of recently published temperature-accelerated lifetime experiments (ALT).^{7–9} These experiments are generally conducted within a controlled environment of a nitrogen-filled dark chamber in an effort to eliminate oxygen/moisture contamination and photo-degradation. Lifetime projection from these ALT experiments is carried out in the literature by empirical extrapolation,^{7,11} but our degradation model interprets these experiments within a common physical framework and relates the projected lifetime with the intrinsic material properties and kinetics of phase segregation.

Before discussing the thermal degradation of BH-OPV in detail, let us briefly review its structure and working principle. Unlike conventional solar cells (e.g., a-Si, CdTe), the active layer of BH-OPV cell [Figs. 1(a) and 1(b)] contains two organic semiconductors (electron donor (D) and electron acceptor (A)), and the interface between them is randomly dispersed throughout the bulk of cell. The distributed cell morphology ensures that regardless of the origin of an exciton, it finds an interface within the diffusion length ($L_{ex} \approx 5\text{--}10\text{ nm}$) and dissociates into charge carriers. For further details, see excellent review articles in Refs. 12–14.

Phase segregation of two organic materials is the key process in the fabrication of BH solar cell. The general characteristics of phase segregation and its relevance for high-performance OPV design are well known to the community.¹⁵ Here we describe the physics of phase segregation during fabrication as well as during operating/stress conditions by the Flory-Huggins’s mean field theory coupled with Cahn-Hilliard (C-H) equation.¹⁶ Detailed discussion on the formulation of free energy and the numerical scheme to solve the C-H equation is explained in Refs. 17 and 18. In Fig. 1 we show the numerical simulation results of such morphology evolution during fabrication [Fig. 1(a)] and ALT stress conditions [Fig. 1(b)]. The figures illustrate that even though the geometry of the meso-structure lacks any specific order/shape, it is still characterized by an average domain width, $\langle W_C \rangle$, that increases systematically with anneal/stress

^{a)}Electronic mail: biswajit.025@gmail.com.

^{b)}Electronic mail: alam@purdue.edu.

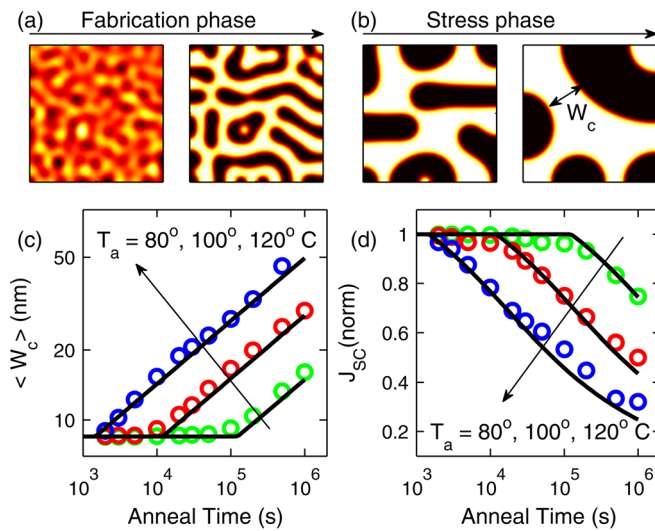


FIG. 1. (Color online) Numerical simulation of the evolution of active layer morphology. (a) During the fabrication step (b) during the thermal stress experiment. (c) The growth of the average domain size ($\langle W_c \rangle$) with the stress time is plotted (log-log plot) for different stress temperatures. We note W_c follows a power law with stress time. (d) Normalised short-circuit current for different stress temperatures are plotted from both numerical simulation (solid lines) and analytical relation [Eq. 2(a)] (symbols).

time t_a . This domain growth/coarsening is known as Ostwald ripening^{16,19} and is given by

$$\langle W_c(t_a, T_a) \rangle \propto [D_{eff}(T_a)t_a]^n. \quad (1)$$

Here D_{eff} is the effective diffusivity of organic/polymer material and n is the “Lifshitz-Slyozov” power exponent^{16,19} associated with spinodal decomposition.

The crux of the intrinsic stability problem in BH-OPV is that the phase separation continues even in the normal operating condition, resulting in time-dependent evolution towards suboptimal morphology and performance degradation with time^{20,21} [see Fig. 1(b)]. As a result, there is a monotonic reduction of J_{SC} (and corresponding loss in efficiency) with operating time (see Ref. 22 for rigorous derivation), as follows:

$$J_{SC}(t) \propto \frac{2L_{ex}}{\langle W_c(t) \rangle} \tanh\left\{\frac{\langle W_c(t) \rangle}{2L_{ex}}\right\} \quad (2a)$$

$$\approx 2L_{ex}/\langle W_c(t) \rangle; \quad \text{for } \langle W_c \rangle \gg L_{ex}, \quad (2b)$$

Combining Eqs. 1 and 2(b), we find that

$$\frac{J_{SC}(t_0 + t_s)}{J_{SC}(t_0)} = \frac{\langle W_c(t_0) \rangle}{\langle W_c(t_0 + t_s) \rangle} = \frac{[D_{eff}(T_0)t_0]^n}{[D_{eff}(T_0)t_0 + D_{eff}(T_s)t_s]^n}. \quad (3)$$

Here t_0 and T_0 represent the anneal time and temperature during the fabrication while t_s and T_s denote the anneal time and temperature during the stress (or operation) phase, respectively. Thus, $J_{SC}(t_0)$ is the short-circuit current of a BH-OPV cell immediately after fabrication, but before it has been put to use or stressed in ALT test. Eq. 3 suggests that J_{SC} begins to decay as soon as the cell is subjected to the stress conditions. The temperature dependence of the J_{SC} degradation is encapsulated in Eq. 3 via the Arrhenius activation of effective mutual diffusivity of the donor and

acceptor materials, i.e., $D_{eff} = D_0 e^{-E_A/kT}$, where D_0 is the maximum diffusivity and E_A is the activation energy of the diffusion process. With temperature-activated diffusion, from Eq. 3 we obtain

$$\hat{J}_{SC}(t_s) = \left(1 + e^{-E_A/kT_s} \left(\frac{t_s}{t_{eq}}\right)\right)^{-n}. \quad (4)$$

Here $\hat{J}_{SC}(t_s) = \frac{J_{SC}(t_0 + t_s)}{J_{SC}(t_0)}$ is the normalized short-circuit current and $t_{eq} (\equiv t_0 e^{-E_A/kT_0})$ is the “equivalent-anneal time” which translates the actual anneal time t_0 to specific stress conditions and it reflects the fabrication conditions of the solar cell. The other two parameters in our model: “Lifshitz-Slyozov” power exponent n and activation energy E_A of the polymer blend are material dependent physical constants. It is observed experimentally that the decay in J_{SC} saturates to a fixed value \hat{J}_{SC}^{sat} , independent to the stress conditions⁷ (in Fig. 2(a), $\hat{J}_{SC}^{sat} \approx 0.4$). We account for this saturation current by an empirical cut-off of $\hat{J}_{SC}(t_s) = \hat{J}_{SC}^{sat}$ for $t_s \geq t_s^*$, where t_s^* is the stress time corresponding: $\hat{J}_{SC}(t_s^*) = \hat{J}_{SC}^{sat}$. More work is needed to model this saturation current, which relates the limit of phase segregation with an attainment of stabilized morphology. Note that while many researchers^{7,8,20} have suggested that phase segregation might play an important role in dictating intrinsic stability of OPV, the specific form of Eq. 4 would now allow accurate lifetime projection and quantitative comparison among results from different groups.

We verify the growth law [Eq. 1] and the dependence of J_{SC} on $\langle W_c \rangle$ [Eq. 2(b)] in Figs. 1(c) and 1(d), respectively, by detailed numerical simulation. We calibrate the model parameters (E_A , n , t_{eq}) by fitting Eq. 4 to a single set of measured polymer degradation data corresponding to a particular stress temperature and use the extracted parameters to predict the J_{SC} degradation at all other temperatures. Figure 2(a) shows a good fit between the model prediction from Eq. 4 and the measured data (MDMO-PPV:PCBM system, Ref. 7). We also observe excellent match between the same model and the measured current for many other data reported in the literature involving different polymer systems (P3HT:PCBM, PPV:PCBM, in Fig. 2(b)). As shown in Fig. 2(c), the extracted values of the material dependent constants: E_A , n , fall in the physical range for the typical OPV materials. We know of no other degradation model that anticipates the intrinsic ALT kinetics of such a broad range of material system. Finally, it is important to note that even though there might be some additional nonthermal intrinsic degradation (like charge accumulation caused by photo-degradation²³), the robustness of n and correlation between the extracted E_A and known bulk E_A of the respective materials assures that morphological effect is the primary source of thermal degradation in these sets of experiments.

Equation 4 can now be used to determine the intrinsic lifetime (t_{life}) of BH-OPV due to thermal degradation, based on the criterion that $J_{SC}(t_0 + t_{life}) = \delta_{tol} J_{SC}(t_0)$; where δ_{tol} is the technology specific tolerance limit for J_{SC} degradation. In other words,

$$t_{life}(T_{op}) = \frac{t_{eq}}{k_{deg}(T_{op})} \left(\delta_{tol}^{-\frac{1}{n}} - 1 \right). \quad (5)$$

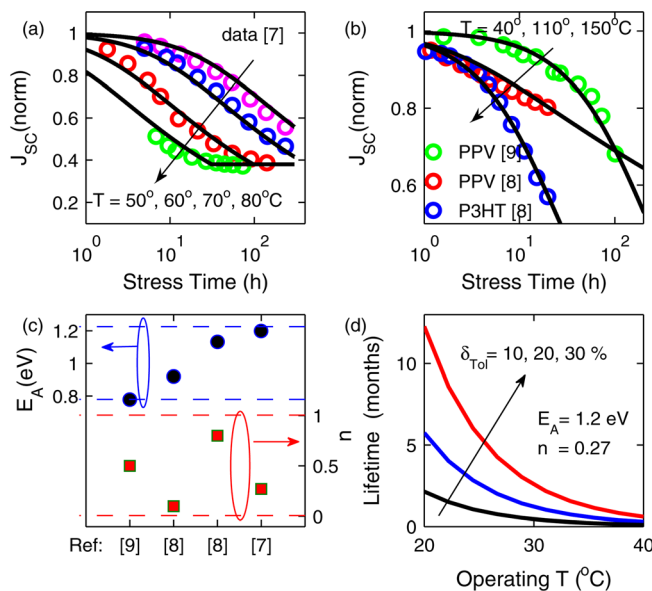


FIG. 2. (Color online) Validation of degradation model (solid line) with measured data (symbols) from literature. (a) Measured J_{SC} degradation values (MDMO-PPV:PCBM cells⁷) matched with model [Eq. 4] for four different stress temperatures. (b) Model validation for other various polymer systems reported in literature.⁷⁻⁹ (c) Power exponent (n) and activation energy (E_A) values described in the model are extracted by fitting the model with the different experimental data set. (d) Model predicted intrinsic lifetime of the cell is plotted for three different tolerance limits in the degradation of J_{SC} .

Here, T_{op} is the operating temperature for the solar cell. In Fig. 2(d) we plot the dependence of the intrinsic lifetime of BH-OPV on the operating temperature for three different tolerance limits δ_{tol} . The figure shows even under the optimistic scenario of very low time exponent, $n \sim 0.27$ and high activation energy $E_A = 1.2$ eV; the cell is predicted to degrade more than 10% within a few months. This provides a simple physical explanation of empirically observed poor stability of organic solar cells. It is important to note that these specific numerical values of lifetime are defined by the polymer systems discussed in Fig. 2(a). As processing conditions improve or as new polymers are developed, the lifetime will certainly increase (see Ref. 2 for recent examples of >1 year lifetime); we suggest however that the intrinsic degradation and lifetime projection will still be defined by Eqs. 4 and 5.

The model discussed above also rationalizes various empirical approaches to improve BH-OPV stability based on kinetic trapping²⁴⁻²⁶. For example, the BH-OPV cells based on block copolymers²⁴ (e.g., PvDMTPA-b-PPerAcr di-block copolymers), where fixed block length prevents phase separation improve intrinsic stability. Similarly, the use of photocrosslinkable copolymers²⁵ or polymerizable fullerene derivative²⁶, where morphology remains stabilized by cross-linking, offers considerable improvement in lifetime. Both these solutions confirm that phase segregation is a dominant stability concern. These solutions are based on kinetically trapped phases that can be understood by Eq. 4 as having higher activation energy E_A following cross-linking. Indeed, the saturation of the J_{SC} degradation with stress time as shown in Fig. 2(a) might also imply a stress-related kinetic trapping of phase segregation, correlated with the attainment of the equilibrium morphology.

If the equilibrium morphology of the polymer based cell can be engineered very close to the optimal morphology ($W_C^{sat} \approx 2L_{ex}$), then the intrinsic stability limit of BH-OPV cell can be extended considerably. Finally, the stability model [Eq. 4] suggests an interesting performance-stability tradeoff inherent in classical BH-OPV structures. Since performance degrades rapidly for an (efficiency) optimized cell, it is clear that slight *under* (suboptimal) processing of the polymer mixture can improve the lifetime of the cell significantly. Such cells will have slightly lower efficiency initially, but during operation the cell performance will improve and thereby extend the intrinsic lifetime significantly. Reference 8 shows a highly suggestive evidence of the viability of such approach.

We have developed a compact physical degradation model for BH-OPV based on theory of spinodal decomposition and morphological evolution. The model predicts intrinsic lifetime of the cell as a function of material parameters and process conditions, and we have validated the model [Eq. 4] against available experimental data. This model not only anticipates projected lifetime of BH-OPV, but also suggests/rationalizes various approaches for the improvement of intrinsic lifetime and performance-stability optimization of organic solar cell.

We gratefully acknowledge financial support from the DOE-ERFC at Columbia (#DE SC0001085) and computational resources from NSF-NCN Center at Purdue (EEC 0228390).

- ¹See <http://www.solarmer.com/> for more information about OPV efficiency.
- ²S. A. Gevorgyan *et al.*, *Sol. Energy Mater. Sol. Cells* **92**, 685 (2008).
- ³F. C. Krebs, *Sol. Energy Mater. Sol. Cells* **92**, 685 (2008).
- ⁴E. Voroshazi, B. Verreert, T. Aernouts, and P. Heremans, *Sol. Energy Mater. Sol. Cells* **95**, 1303 (2011).
- ⁵T. Tromholt, E. A. Katz, B. Hirsch, A. Vossier, and F. C. Krebs, *Appl. Phys. Lett.* **96**, 073501 (2010).
- ⁶B. H. Cumpston and K. F. Jensen, *J. Appl. Polym. Sci.* **69**, 2451 (1998).
- ⁷B. Conings, S. Bertho, K. Vandewal, A. Senes, J. D'Haen, J. Manca, and R. A. J. Janssen, *Appl. Phys. Lett.* **96**, 163301 (2010).
- ⁸S. Bertho *et al.*, *Sol. Energy Mater. Sol. Cells* **92**, 753 (2008).
- ⁹R. de Bettignies *et al.*, in *Organic Photovoltaics V*, edited by Z. H. Kafafi and P. A. Lane (SPIE, Denver, CO, USA, 2004), pp. 216–223.
- ¹⁰S. Sarkar, J. H. Culp, J. T. Whyland, M. Garvan, and V. Misra, *Org. Electron.* **11**, 1896 (2010).
- ¹¹S. Schuller, P. Schilinsky, J. Hauch, and C. J. Brabec, *Appl. Phys. A: Mater. Sci. Process.* **79**, 37 (2004).
- ¹²S. R. Forrest, *MRS Bull.* **30**, 28 (2005).
- ¹³C. Deibel and V. Dyakonov, *Rep. Prog. Phys.* **73**, 096401 (2010).
- ¹⁴A. C. Mayer, S. R. Scully, B. E. Hardin, M. W. Rowell, and M. D. McGehee, *Mater. Today* **10**, 28 (2007).
- ¹⁵H. Hoppe and N. S. Sariciftci, *J. Mater. Chem.* **16**, 45 (2006).
- ¹⁶P. G. de Gennes, *J. Chem. Phys.* **72**, 4756 (1980).
- ¹⁷G. A. Buxton and N. Clarke, *Phys. Rev. B* **74**, 085207 (2006).
- ¹⁸B. Ray, P. Nair, R. Garcia, and M. Alam, in *IEEE International Electron Devices Meeting (IEDM)* (IEEE, Baltimore, MD, 2009), pp. 1–4.
- ¹⁹I. Lifshitz and V. Slyozov, *J. Phys. Chem. Solids* **19**, 35 (1961).
- ²⁰X. Yang, J. K. J. van Duren, R. A. J. Janssen, M. A. J. Michels, and J. Loos, *Macromolecules* **37**, 2151 (2004).
- ²¹J. Jo, S. Kim, S. Na, B. Yu, and D. Kim, *Adv. Funct. Mater.* **19**, 866 (2009).
- ²²B. Ray, P. Nair, and M. A. Alam, in *Photovoltaic Specialists Conference*, (IEEE, Honolulu, Hawaii, 2010), pp. 85–89.
- ²³K. Kawano and C. Adachi, *Adv. Funct. Mater.* **19**, 3934 (2009).
- ²⁴M. Sommer *et al.*, *Adv. Funct. Mater.* **17**, 1493 (2007).
- ²⁵B. J. Kim *et al.*, *Adv. Funct. Mater.* **19**, 2273 (2009).
- ²⁶M. Drees *et al.*, *J. Mater. Chem.* **15**, 5158 (2005).